Silica-Promoted Diels−Alder Reactions in Carbon Dioxide from Gaseous to Supercritical Conditions

Randy D. Weinstein,[†,||] **Adam R. Renslo,**[‡] **Rick L. Danheiser,**[‡] **and Jefferson W. Tester***[,†,§]

Departments of Chemical Engineering and Chemistry and Energy Laboratory, Massachusetts Institute of Technology, Cambridge, Massachusetts 02139

Received: October 27, 1998

Amorphous fumed silica (SiO_2) was shown to increase yields and selectivities of several Diels−Alder reactions in gaseous and supercritical CO_2. Pressure effects on the Diels−Alder reaction were explored using methyl vinyl ketone and penta-1,3-diene at 80 °C. The selectivity of the reaction was not affected by pressure/density. As pressure was increased, the yield decreased. At the reaction temperature, adsorption isotherms at various pressures were obtained for the reactants and the Diels−Alder adduct. As expected when pressure is increased, the ratio of the amount of reactants adsorbed to the amount of reactants in the fluid phase decreases, thus causing the yield to decrease. The Langmuir adsorption model fit the adsorption data. The Langmuir equilibrium partitioning constants all decreased with increasing pressure. The effect of temperature on adsorption was experimentally determined and traditional heats of adsorption were calculated. However, since supercritical CO_2 is a highly compressible fluid, it is logical to examine the effect of temperature at constant density. In this case, entropies of adsorption were obtained. The thermodynamic properties that influence the real enthalpy and entropy of adsorption were derived. Methods of doping the silica and improving yields and selectivities were also explored.

Introduction

The development of "environmentally friendly" chemical processes has been a subject of increasing interest in recent years.[1] One major goal of studies in this area has been the identification of environmentally benign reaction solvents, with considerable attention focusing on the potential utility of supercritical carbon dioxide ($scCO_2$) as a medium for performing important synthetic reactions.[2] Although a number of standard synthetic transformations have been demonstrated to proceed uneventfully in $scCO_2$, to date there have been relatively few reports of reactions that exhibit dramatic rate enhancement or selectivity changes when carried out in supercritical carbon dioxide. Hrnjez et al. observed a modest pressure effect on the stereochemical course of the photochemical dimerization of isophorone in $scCO_2$,[3] and Weedon and co-workers have observed an interesting increase in the ratio of rearrangement to cage-escape products in the photo-Fries rearrangement of naphthyl acetate in near critical CO_2.[4] Noyori and co-workers have shown that the homogeneous catalytic hydrogenation of CO_2 to formic acid and its derivatives proceeds significantly faster in $scCO_2$ (in the presence of a cosolvent) than in traditional liquid solvents.[5] Although carbon dioxide has not yet been shown to provide dramatic advantages over conventional solvents with respect to improved reaction rates and selectivites, the potential environmental and economic advantages of $scCO_2$ continue to fuel interest in this area.

A significant obstacle to the application of $scCO_2$ as a reaction solvent is the fact that the solubility of many common reagents and reactants is impractically low in carbon dioxide. The solvating ability of high-density carbon dioxide is often compared to that of nonpolar organic solvents such as hexane, carbon tetrachloride, and fluorocarbon.[2c] Recent studies aimed at improving the solubility of materials in CO_2 include Johnston's investigation of water in carbon dioxide microemulsions[6] and DeSimone et al.'s work on self-assembled micelles of block copolymer amphiphiles.[7] The use of phase transfer catalysis has also been explored to improve the solubility of some materials in CO_2.[8] Curran and co-workers[9] have recently used fluorinated alkylstannanes to mediate radical cyclization, coupling, and reduction reactions in $scCO_2$, and Burk et al.[10] have reported the rhodium-catalyzed asymmetric hydrogenation of enamides in supercritical carbon dioxide.

In addition to the solubility issues discussed above, a second limitation in performing synthetic reactions in $scCO_2$ is that many standard organic transformations suffer from impractically slow reaction rates in carbon dioxide as compared to conventional organic solvents.[11] While resorting to various Lewis acid promoters might provide a remedy to this problem, the use of such additives would greatly diminish the environmental benefits associated with the use of $scCO_2$. For this reason, we have investigated the use of environmentally benign, reusable solids such as silica and alumina as promoters for organic reactions in $scCO_2$. Among the many attractive features of these materials are their low cost, minimal environmental impact, easy separation from CO_2, and potential for reuse. In this paper we report on the use of amorphous silica (SiO_2) as an environmentally benign promoter for the Diels−Alder reaction in $scCO_2$.

The use of silica to promote reactions including ozonolyses, alkylations, acylations, cycloadditions, halogenations, oxidations, and reductions in traditional organic solvents is well-known.[12] Although these reactions can be carried out on solid silica surfaces without the need for a solvent, extraction with an

---

* Corresponding author. Phone (617) 253-3401. Fax: (617) 253-8013. E-mail: testerel@mit.edu.

† Department of Chemical Engineering.

|| Current address: Department of Chemical Engineering, Villanova University, Villanova, PA 19085.

‡ Department of Chemistry.

§ Energy Laboratory.

organic solvent is still required in order to recover the products from the solid silica phase at the conclusion of the reaction. The use of "doped" silica and alumina to promote reactions in organic solvents has also been reported. For example, Kropp and co-workers[13] have used silica in combination with protic acids to promote a variety of reactions in solvents such as dichloromethane. A solid-phase promoter composed of silica-supported ZnCl$_2$ and alumina-supported K$_2$CO$_3$ has recently been employed for Friedel−Crafts allylation of aromatic rings in dichloroethane.[14]

Despite this considerable body of literature, the use of silica or alumina to promote reactions in scCO$_2$ has not been previously reported. Very recently, Poliakoff and co-workers reported Friedel−Crafts[15] and hydrogenation[16] reactions in scCO$_2$ using sulfonylated polysiloxane and polysiloxane-supported palladium promoters, respectively. These reactions involve the use of gaseous reagents (propene and hydrogen), thereby taking advantage of the high solubility of these gases in scCO$_2$. Compared to the polysiloxane polymers used in this work, silica is significantly less expensive and more readily available.

The aim of the investigation reported herein was to explore temperature and pressure/density effects on the silica-promoted Diels−Alder reaction in CO$_2$. To characterize the reaction system, the partitioning of species between solid and fluid phases was first determined as a function of operating conditions and then models for the adsorption process were developed. The application of protic and Lewis acid dopants to further enhance reaction rates was also explored.

Experimental Section

Materials. Isoprene, methyl vinyl ketone, methyl acrylate, penta-1,3-diene, and acrylonitrile were purified by distillation and stored at −10 °C until use. Cyclopentadiene was prepared by thermal cracking of the dimer and was stored at −60 °C until use. Amporphous fumed silica (Alfa Aesar) with a surface area of 400 m^2/g was dried at 200 °C to constant weight and sealed in a vial under a CO$_2$ atmosphere. Grade 5 CO$_2$ was purchased from BOC Gases. Doped silica was prepared by charging a round-bottomed flask with 25 g of dried silica and 70 mL of dichloromethane and stirring at room temperature while 40 mmol of the dopant (either phosphoric acid, sulfuric acid, AlCl$_3$, or TiCl$_4$) was added dropwise over 2 min. The resulting suspension was stirred for 30 min and then concentrated by rotary evaporation and then at 0.1 mmHg for 2 h to provide material with ca. 1.35 mmol dopant per gram of silica.

Instrumentation. ^{1}H NMR spectra were recorded on Varian XL-300 and Unity 300 spectrometers using a delay time of 10 s. Gas chromatographic analyses were performed on a Hewlett-Packard 6890 gas chromatograph with an auto injector, FID detector, and BD WAX (J&W Scientific) column. All GC data reported are the result of averaging at least three measurements.

Reactor. All CO$_2$ experiments were performed in 25-mL stainless steel view cell reactors described previously.[11b] Agitation was provided by a magnetic stirbar. A six-way sample valve allowed for sampling of the fluid phase of the vessel, and control experiments were carried out to verify the validity of the sampling procedure.

Representative Procedure for Diels−Alder Reactions in Carbon Dioxide. Samples of 3.75 mmol of the diene and 2.5 mmol of the dienophile were sealed in separate oven-dried glass ampules. The ampules, a magnetic stirbar, and 0.50 g of silica were placed in the reactor, which was sealed, placed on a stirplate, and wrapped with heating tape. Low-pressure carbon

dioxide was passed through the system while the temperature was raised to the desired reaction temperature. The reactor was then pressurized, causing the ampules to burst. At the conclusion of the experiment, the contents of the reaction vessel were released slowly through a long narrow tube whose end was immersed in ca. 70 mL of ethyl acetate. Additional ethyl acetate (30 mL) was used to rinse the inside of the reactor and the sampling tubing, and the silica remaining in the reactor was transferred to the ethyl acetate solution. Approximately 100 mL of ethyl acetate was used for the collection process; dichloromethane could also be used as a collection solvent with no effect on the results. Control experiments verified that the quantity of solvent used was sufficient to desorb all materials from the solid silica surface. The combined ethyl acetate solution was passed through a 0.2 μm filter, dried over MgSO$_4$, filtered, and concentrated by rotary evaporation (at ca. 20 mmHg). *p*-Dimethoxybenzene was used as an internal standard for ^{1}H NMR analysis of the products in CDCl$_3$. In the case of experiments carried out at pressures of 0−33 bar, reactants were placed directly into the reactor since at these pressures the glass ampules would not burst.

Representative Phase Distribution Experiments. Various ratios of solid silica and a reactant or cycloadduct were prepared as described above. The reactor vessel was sealed, heated, and pressurized. After 6−8 h, a six-way sample valve was used to remove a 0.5 mL of sample from the fluid phase of the reaction medium. For each experiment, two samples were taken, and the second was deemed to be more representative of the fluid environment. The sample was depressurized by releasing the contents of the 0.5 mL sample loop through a long narrow tube whose end was immersed in diethyl ether. For volatile components (methyl vinyl ketone and penta-1,3-diene), the ether used for collection was cooled by an acetone−dry ice bath to aid in recovery. Tests without silica present were performed to ensure that greater than 95% recovery of all chemicals occurred. The sample loop was washed with ether and low-pressure CO$_2$. To prevent silica particles from clogging the inlet to the sample valve, stirring was terminated just prior to taking a sample, thus allowing the particles to settle away from the inlet to the sample valve. Analysis was performed by GC FID. Equilibrium was verified by taking another sample 24 h later. With the known amount of solvent used for collection, the known volumes of the sample loop and the reactor, and the GC results, the amount of the material in the CO$_2$ phase could be obtained. The amount of species on the silica was calculated by a material balance because this phase could not be sampled.

Results and Discussion

Silica-Promoted Diels−Alder Reactions. Table 1 summarizes the results of our initial investigation of silica-promoted Diels−Alder reactions in carbon dioxide. All of these reactions were performed at 1500 psi (103 bar) in scCO$_2$. In the case of reactions employing cyclopentadiene as diene, cycloadditions were carried out for 4 h at 50 °C. Reactions using penta-1,3-diene and isoprene were performed at 80 °C for 24 h. In all cases, 3.75 mmol of diene and 2.5 mmol of dienophile were used as feed, and 0.5 g of silica was used in experiments involving this material as a reaction promoter.

As shown in Table 1, the use of silica in scCO$_2$ led to increased yields in a number of Diels−Alder reactions. In all cases, an increase in selectivity (favoring the ortho or para regioisomer over the meta isomer and/or the endo stereoisomer over the exo isomer) was observed. The exact mechanism of these silica promotion effects is not well understood.[17] Silica

2880 *J. Phys. Chem. B, Vol. 103, No. 15, 1999*

Weinstein et al.

TABLE 1: Yields and Selectivities of Diels−Alder Reactions in Supercritical Carbon Dioxide with and without Silica Present

entry	conditions[a]	promoter[b]	yield (%)[c]	selectivity[d]
W = COMe				
1	CO$_2$, 50 °C, 4 h	no	29	82:18[e]
2	CO$_2$, 50 °C, 4 h	yes	82	92:8[e]
W = CN				
3	CO$_2$, 50 °C, 4 h	no	5	57:43[e]
4	CO$_2$, 50 °C, 4 h	yes	14	59:41[e]
W = CO$_2$Me				
5	CO$_2$, 50 °C, 4 h	no	5	72:28[e]
6	CO$_2$, 50 °C, 4 h	yes	21	85:15[e]
7	CO$_2$, 80 °C, 24 h	no	5	85(72:28):15(66:33)[f]
8	CO$_2$, 80 °C, 24 h	yes	35	92(87:13):8(76:24)[f]
W = COMe				
9	CO$_2$, 80 °C, 24 h	no	5	67:33[g]
10	CO$_2$, 80 °C, 24 h	yes	35	73:27[g]
W = CO$_2$Me				
11	CO$_2$, 80 °C, 24 h	no	2	68:32[g]
12	CO$_2$, 80 °C, 24 h	yes	3	73:27[g]

[a] All reactions were conducted at 103 bar in CO$_2$. [b] 0.5 g of SiO$_2$ (400 m^2/g). [c] Yield estimated by ^{1}H NMR. [d] Ratios of isomers determined by ^{1}H NMR analysis except for entries 3 and 4 (GC analysis). [e] Endo:exo. [f] Ortho(endo:exo):meta(endo:exo). [g] Para:meta.

promotion of the Diels−Alder reaction probably involves hydrogen bonding to (or protonation of) the dienophile by acidic SiOH groups on the silica surface, thereby lowering the energy of the LUMO$_{dienophile}$ and facilitating the cycloaddition. However, it is unlikely that the observed rate and selectivity enhancements are due solely to the presence of Lewis acid sites on silica surfaces, since these sites are rarely found on the surface of untreated silica.[18] Vesselovskii et al.[19] have proposed that the adsorption of reactants on the surface of silica particles may facilitate the formation and stabilization of prereaction complexes by bringing the reacting moieties within each reactant into closer proximity. A related theory has been advanced by Menger,[20] suggesting that the rigid anchoring of functional groups can fix reactants in proximity to each other less than the critical bonding distance, thus leading to significant rate enhancements. An alternative theory introduced by Parlar and Baumann[21] suggests that only a small fraction of reactants are actually strongly adsorbed on the silica surface and that the enhanced rates and selectivities are caused by symmetry-controlled secondary orbital interactions between strongly adsorbed species and species that are free to move about on the surface. Experimental evidence has been reported for lateral interactions between adsorbed alkanes and alkenes on silica, which greatly influence the absorption process.[22]

In addition to the adsorbate−adsorbent interactions outlined above, there are additional factors that must be considered when evaluating the results of the silica-promoted Diels−Alder reactions reported in Table 1. Previous theories to account for the promotion of reactions on the surface of silica were developed for processes taking place in the *absence of solvent*. In our system, there is a fluid phase (CO$_2$) present that has its
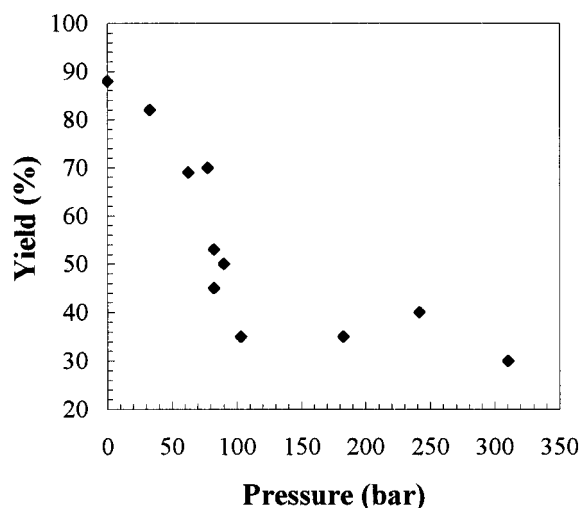

Figure 1. Total yield of the Diels−Alder reaction of methyl vinyl ketone and penta-1,3-diene after 24 h at 80 °C in sub- and supercritical carbon dioxide as a function of pressure with 0.5 g of silica present. The point at 0 bar pressure corresponds to reaction conditions with no CO$_2$ present.

own affinity for the reactants, and consequently, the phase distribution of the reactants and products is expected to be a major factor influencing these reactions. In this connection it should be noted that scCO$_2$ is often used in chromatographic separations because of its ability to alter the partitioning of species from a solid to the supercritical phase. It is also important to note that silica can adsorb CO$_2$ molecules onto its surface,[23] further suggesting that the solvent likely plays a critical role in the adsorption process.

Several studies concerning adsorption from a scCO$_2$ phase onto a solid support have appeared in the literature. Ethyl acetate adsorption equilibria on silica in the presence of scCO$_2$ have been explored,[24] and studies have also been reported on the phase partitioning of sweet orange and lemon essential oils between silica and scCO$_2$.[25] Acetone and benzene adsorption on silica in scCO$_2$ has been examined recently,[26] and activated carbon has been studied as an adsorbent for phenol,[27] toluene,[28] and benzene[29] in the presence of scCO$_2$. In all of these experiments, temperature and pressure were found to have a significant influence on the phase partitioning, consistent with our suggestion that the scCO$_2$ phase plays a significant role in the reactions presented in Table 1. In addition, several infrared spectroscopic studies have revealed how some typical solvents and carbon dioxide are affected when they are adsorbed on the surface of silica in the presence of scCO$_2$.[26,30]

In summary, the rates of our Diels−Alder reactions in the scCO$_2$/SiO$_2$ system are expected to be lower in scCO$_2$ than on the surface of the SiO$_2$ promoter. Any factor that influences the partitioning of reactants between the solid and solution phase could therefore influence the rate of the reaction. The solubility of organic compounds in scCO$_2$ is a strong function of pressure/density, with the solvating power of scCO$_2$ being greater at higher density. Reactions in scCO$_2$ under heterogeneous conditions (i.e., with silica promotion) might therefore be expected to exhibit a pressure effect on reaction rates and yields.

Pressure Effects. The effects of CO$_2$ pressure on the silica-promoted Diels−Alder reaction was examined using the reaction of methyl vinyl ketone and penta-1,3-diene at 80 °C for 24 h. In each experiment, 0.5 g of silica was employed with 3.75 mmol of pentadiene and 2.5 mmol of the ketone. Figure 1 plots the yield of cycloadduct as a function of pressure. As a reference point, note that the critical pressure of CO$_2$ is 74 bar. This
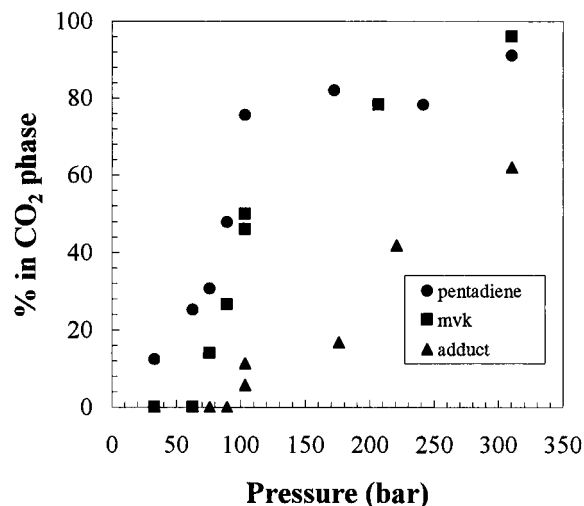
Figure 2. Percent of initial feed amount of methyl vinyl ketone (mvk), penta-1,3-diene, and their Diels−Alder adduct present in the carbon dioxide phase at 80 °C when 2.5 mmol of one of the species is added to 0.5 g of silica in the 25 mL reactor at various carbon dioxide loadings.

Figure 3. Concentration on the solid surface of methyl vinyl ketone (mvk), penta-1,3-diene, and their Diels−Alder adduct at 80 °C when 2.5 mmol of one of the species is added to 0.5 g of silica in the 25 mL reactor at various carbon dioxide loadings.

Diels−Alder reaction was also performed without silica at 1500 psi (103 bar), in which case the isolated yield was only 5% with an ortho(endo:exo):meta(endo:exo) ratio of 85(72:28):15-(66:33). In the case of the silica-promoted reaction, the yield of cycloadduct increases markedly as the pressure is decreased below 100 bar but appears to remain constant at pressures above 100 bar. The stereo- and regioselectivity of the reaction was found to be independent of the system pressure within experimental error and was determined to be 92(87:13):8(76:24), ortho(endo:exo):meta(endo:exo).

As expected, pressure/density has a dramatic effect on the yield of the reaction. This pressure effect is consistent with an increased concentration of reactants on the silica surface at low CO$_2$ pressures (<100 bar) where the solubility of organic compounds in CO$_2$ is low. As the pressure/density of the system is increased, the solubility of organic molecules in the CO$_2$ phase increases[31] and more of the reactants are desorbed from the surface of the silica particles, thus slowing the reaction.

Phase Partitioning Studies. To gain a better understanding of the solvating power of carbon dioxide for each of the reactants and products, we next investigated the phase partitioning of these species under the reaction conditions. Initially, phase distribution experiments were performed using 0.50 g of silica together with either one of the reactants (MVK or pentadiene) or with the product (2.5 mmol; as a mixture of isomers). Procedures for these experiments are described in the Representative Phase Distribution section of the Experimental Section. These reactions were performed at 80 °C at various pressures in order to mimic the reaction conditions employed for the experiments shown in Figure 1. Phase partititoning results for methyl vinyl ketone, penta-1,3-diene, and their Diels−Alder adduct are shown in Figures 2 and 3.

As revealed in these experiments, all of the Diels−Alder adduct remains adsorbed on the surface of the silica until the pressure of the system reaches 100 bar. As the pressure is increased, more adduct is transferred from the solid surface into the scCO$_2$ phase. No maximum in the solubility of this compound in the CO$_2$ phase appears to be reached. Penta-1,3-diene begins to desorb from the surface as soon as some CO$_2$ is added (at the first point of 33 bar); lower pressures could not be examined because reproducible sampling of the fluid phase was not possible. Methyl vinyl ketone begins to desorb at a slightly higher pressure (around the critical pressure of CO$_2$).
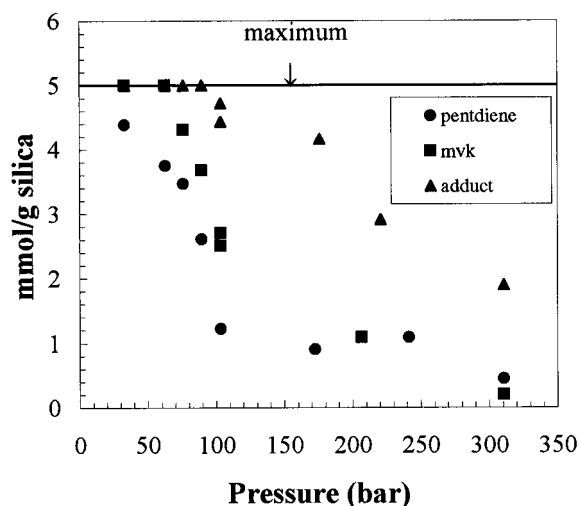
Above 100 bar, the amount of each reactant transferred to the fluid phase appears to level off, and the affinity of these species for the silica surface thus remains fairly constant at pressures above 100 bar.

The observed phase behavior helps to explain the yield data shown in Figure 1. As soon as CO$_2$ is added to the system (at 33 bar), the yield begins to drop off. We attribute this to the fact that penta-1,3-diene is beginning to be removed from the solid surface although the methyl vinyl ketone remains adsorbed. When the reaction is conducted at higher pressures, the yield continues to drop due to the increased desorption of the pentadiene. At pressures above 74 bar, the yield falls even more because the dienophile (MVK) also begins to be desorbed at that point. Finally, when the reaction is carried out at pressures above 100 bar, the amount of the reactants on the surface remains fairly constant with the result that the yield remains constant as pressure is increased.

These phase partitioning experiments reveal that at higher pressures there is a significant portion of the reactants in the fluid phase and not on the surface of the silica particles. The effect of pressure on the rate and selectivity of uncatalyzed, homogeneous Diels−Alder reactions in scCO$_2$ has been previously examined.[11,32] An increase in pressure or fluid density tends to increase the reaction rate and selectivity, but to a lesser degree than that of silica. The fact that the selectivities do not change as a function of pressure suggests that the majority of the reaction is most likely still taking place on the surface of the particles, since if reaction was occurring to a significant extent in the bulk fluid phase, the selectivies would be expected to be lower than we observe.

Adsorption isotherms were next obtained for the reactants and the Diels−Alder adduct in order to better understand the phase behavior of these compounds. Adsorption isotherms were obtained at constant temperature (the reaction temperature of 80 °C) and at constant pressure (several different pressures for each system) by varying the amount of silica and adsorbate fed into the reactor. Procedures for these experiments are described in the Representative Phase Distribution section of the Experimental Section. Constant pressure adsorption isotherms for penta-1,3-diene, methyl vinyl ketone, and their Diels−Alder adduct are shown in Figures 4−6, respectively.

The equilibrium adsorption isotherms clearly indicate that adsorption loading decreases with increases in pressure. This
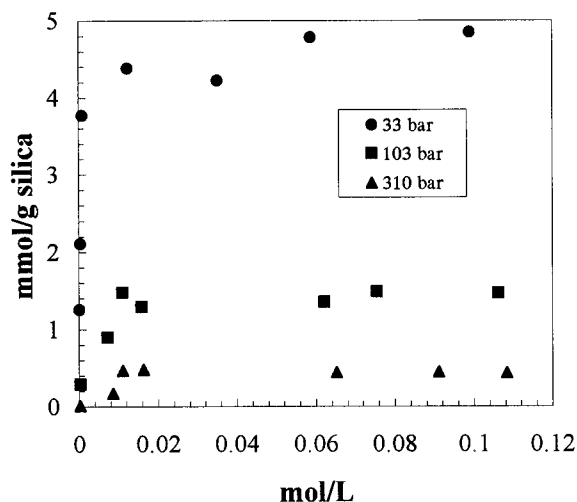
2882 *J. Phys. Chem. B, Vol. 103, No. 15, 1999*

Weinstein et al.

Figure 4. Constant pressure adsorption isotherms for penta-1,3-diene on silica at 80 °C in carbon dioxide.
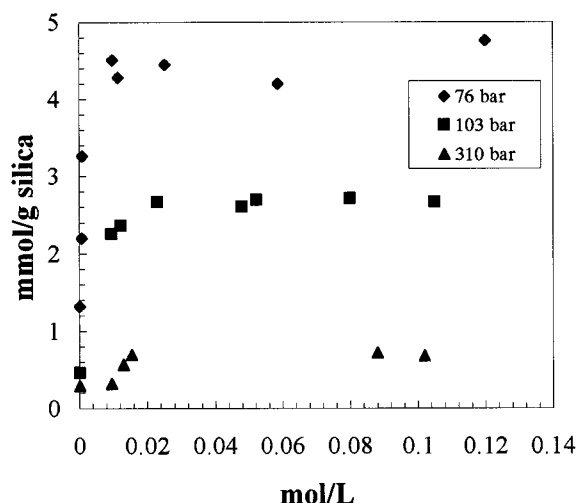

Figure 5. Constant pressure adsorption isotherms for methyl vinyl ketone on silica at 80 °C in carbon dioxide.
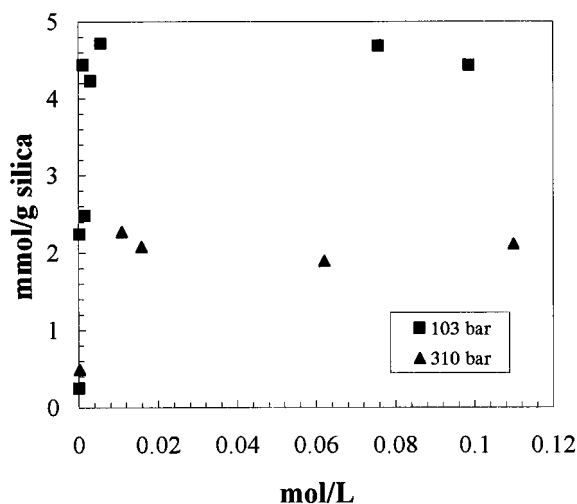

Figure 6. Constant pressure adsorption isotherms for the Diels−Alder adduct of penta-1,3-diene and methyl vinyl ketone on silica at 80 °C in carbon dioxide.

is contrary to the general behavior observed in adsorption from gases near ambient pressure, where the carrier gas is believed to be inert and unaffected by pressure and temperature changes. However, in our systems there is no inert carrier, and the solvent power of CO_2 is greatly affected by pressure and temperature

TABLE 2: Calculated Langmuir K_L and q_∞ Values for Methyl Vinyl Ketone (mvk), Penta-1,3-diene, and Their Diels−Alder Adduct in Carbon Dioxide at 80 °C

pressure (bar)	mvk		pentadiene		adduct	
	K_L (L/mol)	q_∞ (mmol/g)	K_L (L/mol)	q_∞ (mmol/g)	K_L (L/mol)	q_∞ (mmol/g)
33			813	4.9		
76	782	4.7				
103	754	2.7	404	1.5	1892	4.5
310	248	0.7	179	0.5	1432	2.1

changes. Other investigators have also observed changes in the solvent power of CO_2 in adsorption processes.[24,25a,26,28,29,33] There are two interactions that dominate the amount of adsorbed reactant or adduct: (a) the interactions between the adsorbed species, adsorbed CO_2, and silica and (b) the interactions between a dissolved species and CO_2 in the fluid phase. As pressure is increased, the solubility of the species in the fluid phase is increased and more CO_2 is adsorbed on silica. Both of these factors in combination cause the reactant and adduct loadings to decrease as pressure increases. From the adsorption isotherms in scCO₂, it appears that silica has a higher affinity for the adduct over methyl vinyl ketone and penta-1,3-diene. These data may also be interpreted as indicating that CO_2 has a lower affinity for the adduct than the reactants in the presence of silica. Either interpretation of the adsorption processes is reasonable, and the actual process is most likely a combination of the effects.

It was desirable to describe the adsorption isotherms mathematically and there are many models to do this.[34] However, previous investigators[24,28,33b] have found that the Langmuir model fits adsorption data from solutions and CO_2 fairly well and this model was selected. The Langmuir expression is shown in eq 1.

$$\frac{q}{q_\infty} = \frac{K_L C}{1 + K_L C} \tag{1}$$

where q is the amount of adsorbed material, q_∞ is the maximum amount the surface can hold, K_L is the Langmuir equilibrium partitioning constant, and C is the concentration in the bulk CO_2 phase. K_L is equivalent to the initial slope of the adsorption isotherm in terms of mass of solute adsorbed per unit of surface sites available as a function of concentration in the bulk fluid phase. At constant system pressure and temperature, a plot of C/q versus C should give a straight line with slope $m = 1/q_\infty$ and intercept $b = 1/(q_\infty K_L)$. K_L is equal to m/b. The calculated values for K_L and q_∞ are given in Table 2.

In the Langmuir model, K_L and q_∞ can be used to calculate σ^o, the effective area occupied by a molecule on the surface, when the specific area of the solid is known. It is also possible to calculate a heat of adsorption with all the species in their standard states, $\Delta \bar{H}_{L,ads}^+$, for a system that follows the Langmuir model by using eq 2, the van't Hoff equation.

$$\left(\frac{\partial \ln K_L}{\partial (1/T)} \right)_P = -\frac{\Delta \bar{H}_{L,ads}^+}{R} \tag{2}$$

where R is the universal gas constant, T is temperature, and the derivative is taken at constant pressure, P.

We explored the effect of temperature on the adsorption isotherms at 103 bar for penta-1,3-diene and methyl vinyl ketone. The results are shown in Figures 7 and 8, respectively. Figure 9 shows the effect of temperature on the adsorption
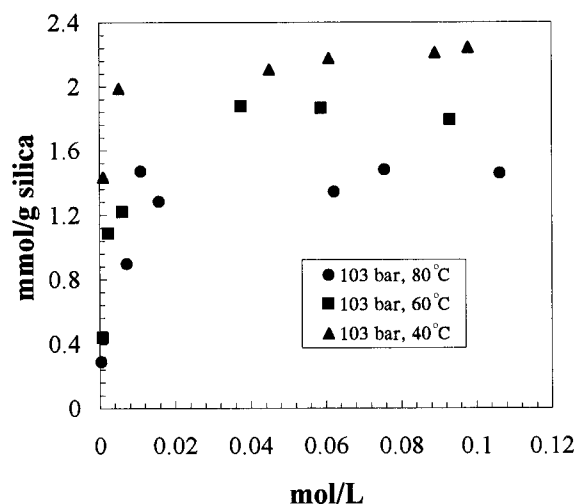
Figure 7. Effect of temperature on the adsorption isotherms for penta-1,3-diene on silica at 103 bar in carbon dioxide.
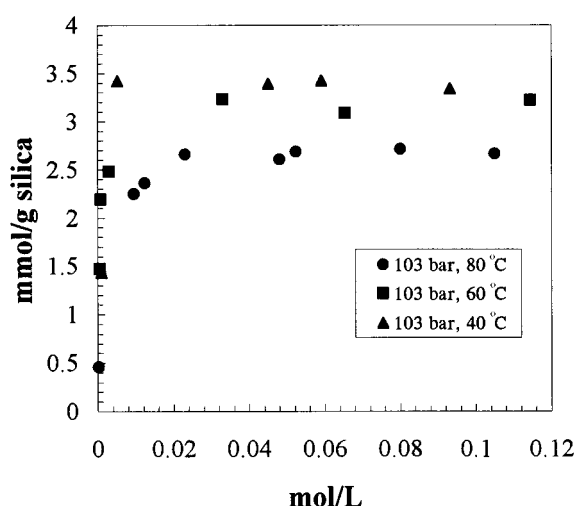

Figure 8. Effect of temperature on the adsorption isotherms for methyl vinyl ketone on silica at 103 bar in carbon dioxide.
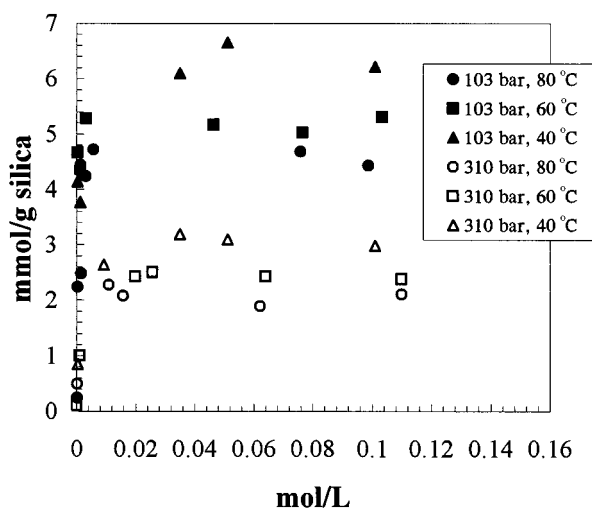

Figure 9. Effect of temperature on the adsorption isotherms for the Diels−Alder adduct of penta-1,3-diene and methyl vinyl ketone on silica at 103 and 310 bar in carbon dioxide.

isotherms for the adduct at 103 and 310 bar. In all cases the equilibrium adsorptive capacity of silica decreases as temperature is increased. Using the data presented in Figures 7−9, the equilibrium adsorption isotherms can be estimated to

TABLE 3: Calculated Langmuir K_L Values for Methyl Vinyl Ketone (mvk), Penta-1,3-diene, and Their Diels−Alder Adduct in Carbon Dioxide at Fixed Pressures

	mvk	pentadiene	adduct	
temp (°C)	K_L (L/mol) at 103 bar	K_L (L/mol) at 103 bar	K_L (L/mol) at 103 bar	K_L (L/mol) at 310 bar
80	754	389	1892	1432
60	1249	526	2886	2366
40	3120	825	9999	5686

TABLE 4: Calculated Values of $\Delta \bar{H}_{L,ads}^+$ (kJ/mol) for Methyl Vinyl Ketone (mvk), Penta-1,3-diene, and Their Diels−Alder Adduct in Carbon Dioxide at Fixed Pressures

mvk at 103 bar	pentadiene at 103 bar	adduct at 103 bar	adduct at 310 bar
−33	−17	−39	−32

TABLE 5: Estimated Values of $\Delta \bar{S}_{L,ads}^+$ (kJ/mol K) for Methyl Vinyl Ketone (mvk), Penta-1,3-diene, and Their Diels−Alder Adduct in Carbon Dioxide at a Fixed Density of 0.6 g/cm³

mvk at 0.6 g/cm³	pentadiene at 0.6 g/cm³	adduct at 0.6 g/cm³
0.07	0.03	0.05

quantify the partitioning of components. These results are shown in Table 3. $\Delta \bar{H}_{L,ads}^+$ at constant pressure is calculated by using eq 2 and is tabulated in Table 4. Both the enthalpy of adsorption and the equilibrium partitioning constants provide similar information about the adsorption process.

However, in scCO$_2$, density has actually been found to be a more representative property than pressure for explaining changes in solubility and phase partitioning.[31] Therefore, it is appropriate to examine the equilibrium constant at conditions of constant density, ρ. Although it is tempting to equate $(\partial \ln K_L/\partial T)_\rho$ with $\Delta \bar{H}_{L,ads}^+$, it is strictly only true for ideal fluids where the enthalpy of mixing is zero and there are no Poynting correction effects between the real state at T and P and the standard states at T and P^+. Variations in the equilibrium partitioning coefficient with temperature are more closely related to the entropy of the process. If we still assume the Langmuir model describes the adsorption process, then
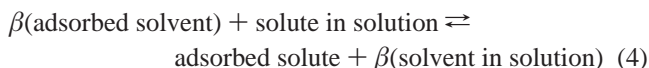
$$R\left(\frac{\partial(T \ln K_L)}{\partial(T)}\right)_\rho = \Delta \bar{S}_{L,ads}^+ \qquad (3)$$

Although adsorption data were not obtained at constant densities, we can still estimate $\Delta \bar{S}_{L,ads}^+$. This was done by interpolating the experimental K_L's at 103 bar and 40 °C (pure CO$_2$ $\rho = 0.6$ g/cm³) from Table 3 and estimating the K_L's at 201 bar and 80 °C (pure CO$_2$ $\rho = 0.6$ g/cm³) from the data in Table 2. When the two K_L's at constant density and different temperature are applied to eq 3, we get a rough estimate of the value of $\Delta \bar{S}_{L,ads}^+$. These estimates are shown in Table 5.

Although the adsorption data can be mathematically reproduced using the Langmuir model (eq 1), the exact physical interpretation of the model parameters is probably not accurate for our system. This can be quickly verified by calculating σ^o from our adsorption isotherms. σ^o is on the order of 10^2 nm² for our species, which is unrealistically large for a monolayer of the reactants or adduct. Most likely, we do not have complete monolayer coverage because the surface of the silica is not homogeneous. The Langmuir model assumes a two-dimensional surface adsorption phase in equilibrium with the bulk fluid solution. The bulk solution may also be assumed to be dilute

2884 *J. Phys. Chem. B, Vol. 103, No. 15, 1999*

Weinstein et al.

and therefore approximated by an ideal solution. Also, adsorbed solvent (CO_2) and solute molecules are assumed to occupy equal areas on a homogeneous surface that is characterized by a single parameter, the fractional coverage, Θ, which varies from 0 to 1. The surface is also believed to be homogeneous. Many of these assumptions are probably not valid in a system where a highly compressible nonideal supercritical fluid is present. Using eqs 2 and 3 for exploring temperature effects of adsorption provides useful scaling information. However, these equations are only approximate representations of the adsorption process, which includes the effects of nonideal solution behavior. In the limit of an ideal solution, eqs 2 and 3 would result, but in the real system significant nonideal interactions need to be included to place physical significance on the adsorption process. This will be done by deriving a more rigorous form of the van't Hoff equation for our system.

At equilibrium, the rate of adsorption equals the rate of desorption. We can consider the process of adsorption and desorption as an equilibrium chemical reaction shown in eq 4 for each species separately.

$$\beta(\text{adsorbed solvent}) + \text{solute in solution} \rightleftharpoons$$
$$\text{adsorbed solute} + \beta(\text{solvent in solution}) \quad (4)$$

where β equals the number of solvent molecules displaced from the surface for each solute molecule that is adsorbed. The equilibrium constant can be written in terms of the species activities, a_i, as

$$K_a = \frac{a_1^{(s)}(a_2^{(b)})^\beta}{(a_2^{(s)})^\beta a_1^{(b)}} \quad (5)$$

where the subscripts denote the species (1 = solute, 2 = CO_2) and the superscripts denote the phase (s = adsorbed solid phase, b = bulk fluid phase). The activity of a species is related to the chemical potential of the species, μ_i, and the chemical potential of the species in its standard state, μ_i^+, by the following:

$$RT \ln a_i = \mu_i - \mu_i^+ \quad (6)$$

At equilibrium at a uniform temperature and pressure,

$$\mu_i^{(b)} = \mu_i^{(s)} \quad (7)$$

and

$$\sum_{1,2} \nu_i \mu_i^{(\pi)} = 0 \quad (8)$$

where ν_i is the stoichiometric coefficient for the reaction shown in eq 4 (reactants are negative and products are positive) and π represents the phase of the species. Thus, the equilibrium constant can now be written as

$$RT \ln K_a = \mu_1^{(s)+} + \beta\mu_2^{(b)+} - \beta\mu_2^{(s)+} - \mu_1^{(b)+} \quad (9)$$

Taking the derivative of both sides of eq 9 with respect to T at constant P, we get

$$-R\left(\frac{\partial \ln K_a}{\partial(1/T)}\right)_P = \bar{H}_1^{(s)+} + \beta\bar{H}_2^{(b)+} - \beta\bar{H}_2^{(s)+} - \bar{H}_1^{(b)+} = \Delta\bar{H}_{ads}^+$$
$$(10)$$

where the "overbar" denotes a partial molar property that is

taken generally to represent the standard state condition of T^+, P^+, and x_i^+ (mole fraction) in each phase π. If the standard states are taken as pure components at T and P of the system, then $x_i^+ = 1$ and the "overbars" are not needed. In addition, it was assumed that β is a constant unaffected by temperature.

By examining eq 10, we can see which terms will affect the adsorption equilibrium as a function of temperature at constant pressure. The traditional heat of adsorption is actually made up of four terms, the partial molar enthalpies of the two species in the two phases following the reaction in eq 4, $\Delta H_{ads} = \bar{H}_1^{(s)} - \bar{H}_1^{(b)} + \beta(\bar{H}_2^{(s)} - \bar{H}_2^{(b)})$. If we assumed the behavior required for the Langmuir model, β would be set to 1. Also, we would have to assume ideal solution behavior so that the activities can be replaced by the mole fractions. The "overbars" may then be dropped because the partial molar enthalpy is just equal to the pure component enthalpy in the ideal solution limit. These assumptions are required to obtain a heat of adsorption from the Langmuir model. Consequently, when supercritical fluids are involved in the process, an unrealistic heat of adsorption would be extracted from the data. This can be shown by relating the concentration-based constant (or continued product of concentrations) to the true activity-based thermodynamic equilibrium constant. The Langmuir model uses a concentration-based partitioning coefficient. The activity coefficient relates activity to concentration directly from its definition:

$$a_i^{(\pi)} \equiv x_i^{(\pi)} \gamma_i^{(\pi)} = \frac{C_i^{(\pi)} \gamma_i^{(\pi)}}{\rho^{(\pi)}} \quad (11)$$

where $\gamma_i^{(\pi)}$ refers to component i in phase π relative to the selected standard state $C_i^{+(\pi)}$, $C_i^{(\pi)}$ is the concentration of species i in phase π (moles of i per liter of fluid for the bulk fluid phase and moles of i per gram of solid for the adsorbed phase), and $\rho^{(\pi)}$ is the molar density of phase π. For the bulk fluid phase, the density is the true molar density of the phase in moles per liter. For the adsorbed phase, it is more convenient to use the maximum amount of i that the surface can hold, $\rho_{max}^{(s)}$, as the "density of the adsorbed phase" for use in an equation of the form of eq 11 for defining the mole fraction in the solid phase, $x_i^{(s)}$. For the adsorbed phase, the mole fraction is more of a percentage of maximum coverage rather than a true mole fraction interpretation. The concentration-based constant is defined as

$$K_C \equiv \frac{C_1^{(s)}(C_2^{(b)})^\beta}{(C_2^{(s)})^\beta C_1^{(b)}} \quad (12)$$

and can be related to the activity-based equilibrium constant given in eq 5 using eq 11.

$$K_C = K_a K_\gamma^{-1}\left(\frac{\rho_{max}^{(s)}}{\rho^{(b)}}\right)^{\beta-1} \quad (13)$$

Here K_γ is defined as the continued product of activity coefficients and is mathematically similar to eq 12 with species concentrations replaced by species activity coefficients. If the solution is ideal in both phases then $K_C = K_a$.

Now we can take the natural log of both sides of eq 13 and then take the partial derivative with respect to temperature at

constant pressure. Again, β was assumed to be a constant independent of temperature.

$$\left(\frac{\partial \ln K_C}{\partial T}\right)_P = \left(\frac{\partial \ln K_a}{\partial T}\right)_P - \left(\frac{\partial \ln K_\gamma}{\partial T}\right)_P +$$
$$(\beta - 1)\left(\frac{\partial \ln \rho_{max}^{(s)}}{\partial T} - \frac{\partial \ln \rho^{(b)}}{\partial T}\right)_P \quad (14)$$

Using eq 10 and noting that the maximum coverage on the solid is constant,

$$\left(\frac{\partial \ln K_C}{\partial T}\right)_P = \frac{\Delta \bar{H}_{ads}^+}{RT^2} - \left(\frac{\partial \ln K_\gamma}{\partial T}\right)_P - (\beta - 1)\left(\frac{\partial \ln \rho^{(b)}}{\partial T}\right)_P \quad (15)$$

In a nonideal system, like ones containing supercritical fluids, it is really the activity-based equilibrium constant that must be used to obtain the true heat of adsorption. Using concentration-based constants, like the ones used in most adsorption models including the Langmuir model, does not produce the heat of adsorption when the derivative of $\ln K_C$ is taken with respect to temperature. Instead, a term that is influenced by the heat of adsorption, the activity coefficients, as well as the density of the bulk phase is obtained. When the bulk phase consists of a supercritical fluid, variations in both activity coefficients and density with changes in temperature are often large, especially near the critical point of the fluid, and consequently, neither can be neglected. A similar approach may be used to show how K_C changes with temperature at constant density.

$$\left(\frac{\partial(T \ln K_C)}{\partial T}\right)_\rho = \frac{\Delta \bar{S}_{ads}^+}{R} - \left(\frac{\partial(T \ln K_\gamma)}{\partial T}\right)_\rho - (\beta - 1) \ln \rho^{(b)} \quad (16)$$
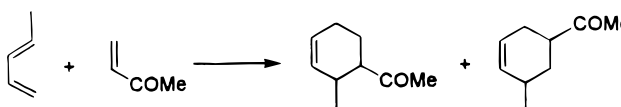
Equations 15 and 16 provide a physical basis for interpreting adsorption behavior. However, since it is often difficult to measure K_C with high precision, an alternative approach for examining phase partitioning in supercritical fluids should be used. It is possible to express variations in the bulk concentration of the solute with respect to temperature, without introducing the concept of an equilibrium constant. This approach is presented in detail in the Appendix, as it deviates from the traditional method of examining adsorption behavior but seems more appropriate when supercritical solvents are present. With an accurate volumetric *PVTN* equation of state and the adsorption data obtained in Figures 7−9, it is possible to estimate true heats of adsorption for the process without actually having to calculate all the activity coefficients and without explicitly using the β term. The final result expresses the derivative of solute concentration as a function of temperature as

$$\left(\frac{\partial x_1^{(b)}}{\partial T}\right)_P = \frac{-x_1^{(s)}(\bar{H}_1^{(s)} - \bar{H}_1^{(b)}) - x_2^{(s)}(\bar{H}_2^{(s)} - \bar{H}_2^{(b)})}{RT^2\left(x_1^{(s)} - \frac{x_2^{(s)} x_1^{(b)}}{x_2^{(b)}}\right)\left(\frac{\partial \hat{f}_1^{(b)}}{\partial x_1^{(b)}}\right)_{T,P}} \quad (17)$$

where the terms in eq 17 are defined in the Appendix.

Doped Silica. We have found the activation provided by untreated silica promoters to be only modest. By comparison, Lewis acid promoted Diels−Alder reactions typically proceed at or below room temperature. The identification of highly activated solid-phase promoters with reactivity comparable to Lewis acids is desirable and we have initiated an investigation of the reactivity of protic and Lewis acid doped silica promoters. To date, we have prepared silica doped with H$_2$SO$_4$, H$_3$PO$_4$,

TABLE 6: Isolated Yields and Selectivities of the Diels−Alder Reaction of Methyl Vinyl Ketone and Penta-1,3-diene with Several Doped and Untreated Silica Promoters

entry	conditions	promoter	yield (%)^a	selectivity^b
1	toluene, 100 °C, 5 d	none	77	82(69:31):18(60:40)
2	no solvent, 25 °C, 0.5 h	SiO$_2$−H$_3$PO$_4$	83	99(93:7):1(N.D.)
3	no solvent, 25 °C	SiO$_2$−H$_2$SO$_4$	c	
4	no solvent, 25 °C	SiO$_2$−AlCl$_3$	c	
5	no solvent, 25 °C	SiO$_2$−TiCl$_4$	c	
6	CO$_2$, 33 bar, 80 °C, 24 h	SiO$_2$	78	92(87:13):8(76:24)
7	CO$_2$, 103 bar, 80 °C, 24 h	SiO$_2$	35	92(87:13):8(76:24)
8	CO$_2$, 103 bar, 40 °C, 4 h	SiO$_2$−H$_3$PO$_4$	57	98(84:16):2(N.D.)

^{a} Isolated yields. ^{b} Selectivity, ortho(endo:exo):meta(endo:exo), was determined by ^{1}H NMR analysis. ^{c} Diene polymerization predominated.

AlCl$_3$, and TiCl$_4$. The reaction of methyl vinyl ketone and penta-1,3-diene was selected as a test case to evaluate the reactivity of these new acid-doped promoters. The reaction was first investigated under solid-phase reaction conditions (no solvent) and then, if successful, the reactions were attempted in scCO$_2$. The results of the initial studies are shown in Table 6.

Phosphoric acid doped silica was found to be an exceptionally effective promoter, producing an 83% isolated yield of cycloadduct after only 30 min at room temperature in the absence of solvent. Furthermore, the regio- and stereoselectivity of the reaction was excellent. When other doped promoters were used in the reaction, violent exotherms developed, and the starting materials decomposed almost immediately. Presumably, cationic diene polymerization is a favorable process under these highly acidic reaction conditions. Apparently, the phosphoric acid promoted cycloaddition is sufficiently accelerated as to be competitive with diene polymerization. In scCO$_2$, the use of SiO$_2$−H$_3$PO$_4$ provides acceptable yields (57%) of Diels−Alder cycloadduct after 4 h at 40 °C. Longer reaction times and higher temperatures did not improve the yield of this reaction. By comparison, the use of untreated silica requires longer reaction times and higher temperatures.

Concluding Remarks

In gaseous and supercritical CO$_2$, the yield and selectivity of several Diels−Alder reactions are enhanced by fumed silica with a high specific area ($\approx$400 m^2/g). Acid doping of silica promoters has been shown to greatly enhance their activating effect. The initial studies with these promoters lay the groundwork for their application to a wide range of other acid and Lewis acid promoted reactions in scCO$_2$. Although the selectivity of these silica-enhanced reactions are not affected by changes in pressure or fluid density, product yields are altered. In general, as pressure is increased, the yield decreases. This was discovered to be caused by the change in concentration of the reactants on the surface of the silica particles. At the reaction temperature, adsorption isotherms were obtained at selected pressures. As expected, when pressure is increased, the ratio of the amount of reactants adsorbed on the silica surface to the amount of reactants in the fluid phase decreases, thus causing the yield to decrease. The Langmuir adsorption model fits the data well, primarily as a result of the decrease in the Langmuir equilibrium partitioning constant that occurs with increasing pressure.

The effect of temperature on the measured Langmuir equilibrium constants was correlated using a traditional heat of

adsorption approach. However, because of the highly nonideal fluid state in this reacting system, the true heat of adsorption for the process in CO_2, $\Delta\bar{H}_{ads}^{+}$, is really a combination of the partial molar enthalpies of the solvent and reactant or product in the CO_2 phase and on the solid surface and can only be obtained when an activity-based equilibrium constant is used. The Langmuir equilibrium constant, although providing useful scaling information, does not physically describe the true process of adsorption in these systems. Since supercritical CO_2 is a compressible dense fluid, the effect of temperature on the equilibrium partitioning constants is more clearly described at a fixed fluid density rather than at a specified constant pressure. At fixed density, one could obtain $\Delta\bar{S}_{ads}^{+}$, from a combination of the partial molar entropies of the solvent and the reactant or product in both phases. Again, the activity-based equilibrium constant must be used. Our work suggests that for adsorbing reacting systems in supercritical fluids it might be best to utilize the standard state reaction free energy, $\Delta\bar{G}_{ads}^{+}$, which is equal to $\Delta\bar{H}_{ads}^{+} - T^{+}\Delta\bar{S}_{ads}^{+}$. Such standard state Gibbs free energies of adsorption capture both pressure and density effects in the reacting system. There is no reason to believe that $\Delta\bar{G}_{ads}^{+}$, $\Delta\bar{H}_{ads}^{+}$, and $\Delta\bar{S}_{ads}^{+}$ are actually constant over a wide range of temperatures and pressures (or fluid densities).

Appendix

Here we present an alternative approach for examining phase distributions of species between a solid surface and a bulk supercritical fluid phase. The true heats of adsorption can be obtained easily with this approach. In a two-component (1 = solute, 2 = CO_2) system with two phases (s = adsorbed solid, b = bulk fluid phase), the Gibbs−Duhem equation can be written independently for each phase.

$$\frac{H^{(s)}}{T^2} dT - \frac{V^{(s)}}{T} dP + \sum_{1,2} x_i^{(s)} d(\mu_i^{(s)}/T) = 0 \qquad (A1)$$

$$\frac{H^{(b)}}{T^2} dT - \frac{V^{(b)}}{T} dP + \sum_{1,2} x_i^{(b)} d(\mu_i^{(b)}/T) = 0$$

With the phase in equilibrium, the chemical potential of each species must be equal in each phase. Thus, $\mu_i^{(s)} = \mu_i^{(b)}$. For a constant pressure case ($dP = 0$), Cramer's rule can be used to simplify eq A1.[35] Using a determinant format, eq A1 becomes

$$\frac{1}{T^2}\begin{vmatrix} H^{(s)} & x_2^{(s)} \\ H^{(b)} & x_2^{(b)} \end{vmatrix} dT + \begin{vmatrix} x_1^{(s)} & x_2^{(s)} \\ x_1^{(b)} & x_2^{(b)} \end{vmatrix} d(\mu_1/T) = 0 \qquad (A2)$$

Now, the total differential of the chemical potential over temperature needs to be expanded. For the constant pressure case it is explicitly expanded as a function of T and x_i. Arbitrarily, choosing the bulk fluid phase (b)

$$d\left(\frac{\mu_1}{T}\right) = d\left(\frac{\mu_1^{(b)}}{T}\right) = \left(\frac{\partial(\mu_1^{(b)}/T)}{\partial T}\right)_{P,x_2^{(b)}} dT +$$

$$\sum_{i=1}^{2} \frac{1}{T}\left(\frac{\partial\mu_1^{(b)}}{\partial x_i^{(b)}}\right)_{T,P,x_j^{(b)}[i,k]} dx_i^{(b)} \quad (A3)$$

The variance of this system ($\diagup$) needs to be evaluated. From the Gibbs phase rule, $\diagup = n + 2 - \pi - r$ where n is the number

of components, π is the number of phases, and r is the total number of reactions and other constraints. In this case $n = 2$, $\pi = 2$, and $r = 1$ (constant P), so $\diagup = 1$. Since we are dealing with a monovariant equilibrium system, variations in chemical potential only need to be examined with respect to one mole fraction parameter. Variations with the other mole fraction term are constrained by the multiphase reaction equilibrium and by the fact that the sum of the mole fractions of any phase must equal unity. We can now apply the Gibbs−Helmholtz equation for the temperature derivative of the chemical potential divided by temperature in eq A3 to produce

$$d\left(\frac{\mu_1}{T}\right) = -\frac{\bar{H}_1^{(b)}}{T^2} dT + \frac{1}{T}\left(\frac{\partial\mu_1^{(b)}}{\partial x_1^{(b)}}\right)_{T,P} dx_1^{(b)} \qquad (A4)$$

Equation A2 can be combined with eq A4 to give the variation of the fluid phase mole fraction with respect to temperature.

$$\left(\frac{\partial x_1^{(b)}}{\partial T}\right)_P = -\frac{\begin{vmatrix} H^{(s)} & x_2^{(s)} \\ H^{(b)} & x_2^{(b)} \end{vmatrix} + \bar{H}_1^{(b)}\begin{vmatrix} x_1^{(s)} & x_2^{(s)} \\ x_1^{(b)} & x_2^{(b)} \end{vmatrix}}{T\begin{vmatrix} x_1^{(s)} & x_2^{(s)} \\ x_1^{(b)} & x_2^{(b)} \end{vmatrix}\left(\frac{\partial\mu_1^{(b)}}{\partial x_1^{(b)}}\right)_{T,P}} \qquad (A5)$$

It is also possible to introduce the fugacity of species 1 in the fluid phase mixture, $\hat{f}_1^{(b)}$, at this point.

$$\mu_1^{(b)} = RT \ln \hat{f}_1^{(b)} + \lambda_1(T) \qquad (A6)$$

where λ_1 is a function that depends on temperature only. Now eq A6 can be used with the following equations to simplify eq A5:

$$H^{(s)} = \sum x_i^{(s)} \bar{H}_i^{(s)}$$
$$H^{(b)} = \sum x_i^{(b)} \bar{H}_i^{(b)} \qquad (A7)$$

which yields,

$$\left(\frac{\partial x_1^{(b)}}{\partial T}\right)_P = \frac{-x_1^{(s)}(\bar{H}_1^{(s)} - \bar{H}_1^{(b)}) - x_2^{(s)}(\bar{H}_2^{(s)} - \bar{H}_2^{(b)})}{RT^2\left(x_1^{(s)} - \frac{x_2^{(s)} x_1^{(b)}}{x_2^{(b)}}\right)\left(\frac{\partial\hat{f}_1^{(b)}}{\partial x_1^{(b)}}\right)_{T,P}} \qquad (A8)$$

Equation A8 contains the true heats of adsorption for the isobaric monovariant system. The change in partial molar enthalpy for each species from the solid phase to the fluid phase is effectively the differential heat of adsorption for that species. With an ideal solution or ideal gas mixture, the composition of each phase as well as the change in the bulk phase composition with respect to temperature at constant pressure is all that is required to calculate the heats of adsorption. In these ideal cases the fugacity can be replaced by the mole fraction of the species times pressure (for ideal gas) or the pure component fugacity (for ideal solution). However, in a nonideal solution, the mixture fugacity must be used, which is given by the continued product of the mole fraction of the species, the pressure of the system, and the fugacity coefficient, $\hat{\phi}_1^{(b)}$. In such nonideal systems, the fugacity coefficient does not equal unity but can be obtained with an appropriate $P\underline{V}TN$ equation of state for the mixture:[35]

$$RT \ln \hat{\phi}_1^{(b)} = -\int_{\infty}^{V} \left(\left(\frac{\partial P}{\partial N_1} \right)_{T,N_2,\underline{V}} - \frac{RT}{\underline{V}} \right) d\underline{V} - RT \ln \left(\frac{PV}{NRT} \right)$$

$$(A9)$$

where N_1 and N_2 are mole numbers.

References and Notes

(1) For example see chapter 1 in Anastas, P. T.; Williamson, T. C. *ACS Symp. Ser.* **1996**, *626*, 1.

(2) (a) Subramaniam, B.; McHugh, M. A. *Ind. Eng. Chem. Process Des. Dev.* **1986**, *25*, 1. (b) Kaupp, G. *Angew. Chem., Int. Ed. Engl.* **1994**, *33*, 1452. (c) Poliakoff, M.; Howdle, S. *Chem. Br.* **1995**, *31*, 118. (d) Savage, P. E.; Gopalan, S.; Mizan, T. I.; Martino, C. J.; Brock, E. E. *AIChE J.* **1995**, *47*, 1723. (e) Black, H. *Environ. Sci. Technol*. **1996**, *30*, 124A. (f) Clifford, T.; Bartle, K. *Chem. Ind*. **1996**, 449. (g) Morgenstern, D. A.; LeLacheur, R. M.; Morita, D. K.; Borowsky, S. L.; Feng, S.; Brown, G. H.; Luan, L.; Gross, M. F.; Burk, M. J.; Tumas, W. *ACS Symp. Ser.* **1996**, *626*, 132.

(3) Hrnjez, B. J.; Mehta, A. J.; Fox, M. A.; Johnston, K. P. *J. Am. Chem. Soc.* **1989**, *111*, 2662.

(4) Andrew, D.; Des Islet, B. T.; Margaritis, A.; Weedon, A. C. *J. Am. Chem. Soc.* **1995**, *117*, 6132.

(5) (a) Jessop, P. G.; Ikariya, T.; Noyori, R. *Nature* **1994**, *368*, 231. (b) Jessop, P. G.; Ikariya, T.; Noyori, R. *Science* **1995**, *269*, 1065. (c) Jessop, P. G.; Hsiao, Y.; Ikariya, T.; Noyori, R. *J. Am. Chem. Soc.* **1996**, *118*, 344. (d) Jessop, P. G. *Top. Catal.* **1998**, *5*, 95.

(6) Johnston K. P.; Harrison, K. L.; Clarke, M. J. Howdle, S. M.; Heitz, M. P.; Bright, F. V.; Carlier, C.; Randolph, T. W. *Science* **1996**, *271*, 624.

(7) McClain, J. B.; Betts, D. E.; Canelas, D. A.; Samulski, E. T.; DeSImone, J. M.; Londono, J. D.; Cochran, H. D.; Wignall, G. D.; Chillura-Matino, D.; Triolo, R. *Science* **1996**, *274*, 2049.

(8) Dillow, A. K.; Yun, S. L. J.; Suleiman, D.; Boatright, D. L.; Liotta, C. L.; Eckert, C. A. *Ind. Eng. Chem. Res.* **1996**, *35*, 1801.

(9) Hadida, S.; Super, M. S.; Beckman, E. J.; Curran, D. P. *J. Am. Chem. Soc.* **1997**, *119*, 7406.

(10) Burk, M. J.; Feng, S.; Gross, M. F.; Tumas, W. *J. Am. Chem. Soc.* **1995**, *117*, 8277.

(11) (a) Weinstein, R. D.; Renslo, A. R.; Danheiser, R. L.; Harris, J. G.; Tester, J. W. *J. Phys. Chem.* **1996**, *100*, 12337. (b) Renslo, A. R.; Weinstein, R. D.; Tester, J. W.; Danheiser, R. L. *J. Org. Chem.* **1997**, *62*, 4530.

(12) Basiuk, V. A. *Russ. Chem. Rev.* **1995**, *64*, 1003.

(13) Kropp, P. J.; Breton, G. W.; Craig, S. L.; Crawford, S. D.; Durland, W. F.; Jones, J. E.; Raleigh, J. S. *J. Org. Chem.* **1995**, *60*, 4246.

(14) Kodomari, M.; Nawa, S.; Miyoshi, T. *J. Chem. Soc., Chem. Commun.* **1995**, 1895.

(15) Hitzler, M. G.; Smail. F. R.; Ross, S. K.; Poliakoff, M. *J. Chem. Soc., Chem. Commun.* **1998**, 259.

(16) Hitzler, M. G.; Poliakoff, M. *J. Chem. Soc., Chem. Commun.* **1997**, 1667.

(17) Veselovskii, V. V.; Gybin, A. S. Lozanova, A. V.; Moiseenko, A. M.; Smit, W. A.; Caple, R. *Tetrahedron Lett*. **1988**, *29*, 175.

(18) (a) Little, L. H. *Infrared Spectra of Adsorbed Species*; Academic Press: New York, 1966. (b) Iler, R. K. *The Chemistry of Silica*; John Wiley and Sons: New York, 1979.

(19) (a) Veselovskii, V. V.; Lozanova, A. V.; Moiseenko, A. M.; Gybin, A. S.; Stim, V. A. *Bull. Acad. Sci. USSR* **1987**, 887. (b) Veselovskii, V. V.; Gybin, A. S. Lozanova, A. V.; Moiseenko, A. M.; Smit, W. A. *Bull. Acad. Sci. USSR* **1990**, 107.

(20) Menger, F. M. *Acc. Chem. Res.* **1985**, *18*, 128.

(21) Parlar, H.; Baumann, R. *Angew. Chem., Int. Ed. Engl.* **1981**, *20*, 1014.

(22) Jagiello, J.; Bandosz, T. J.; Putyera, K.; Schwarz, J. A. *Fundam. Adsor*. **1996**, 417.

(23) (a) Lemcoff, N. O.; Sing, K. S. W. *J. Colloid Interface Sci*. **1977**, *61*, 227. (c) Berlier, K.; Frere, M. *J. Chem. Eng. Data* **1997**, *42*, 533. (b) Olivier, M. G.; Jadot, R. *J. Chem. Eng. Data* **1997**, *42*, 230.

(24) Lochmuller, C. H.; Mink, L. P. *J. Chromatogr.* **1987**, *409*, 55.

(25) (a) Dugo, P.; Mondello, L.; Bartle, K. D.; Clifford, A. A.; Breen, D. G. P. A. *Flavour Fragance J.* **1995**, *10*, 51. (b) Reverchon, E.; Iacuzio, G. *Chem. Eng. Sci.* **1997**, *52*, 3553. (c) Subra, P.; Vega-Bancel, A.; Reverchon, E. *J. Supercrit. Fluids* **1998**, *12*, 43.

(26) Jin, D. W.; Nitta, T.; Park, D. W. *Bull. Chem. Soc. Jpn.* **1997**, *70*, 2987.

(27) Kander, R. G.; Paulaitis, M. E. In *Chemical Engineering and Supercritical Conditions*; Penninger, J. M. L., Gray, R. D., Davidson, P., Eds.; Ann Arbor Science: Ann Arbor, MI, 1983; p 461.

(28) Tan, C. S.; Liou, D. C. *Ind. Eng. Chem. Res.* **1990**, *29*, 1412.

(29) Shojibara, H.; Sato, Y.; Takishima, S.; Masuoka, H. *J. Chem. Eng. Jpn.* **1995**, *28*, 245.

(30) (a) Jin, D. W.; Nitta, T. *J. Chem. Eng. Jpn.* **1996**, *29*, 708. (b) Jin, D. W.; Onose, K.; Fukukawa, H.; Nitta, T.; Ichimura, K. *J. Chem. Eng. Jpn.* **1996**, *29*, 139.

(31) McHugh, M. A.; Krukonis, V. J. *Supercritical Fluid Extraction*, 2nd ed.; Butterworth-Heinemann: Boston, 1994.

(32) Kim, S.; Johnston, K. P. *Chem Eng. Commun.* **1988**, *63*, 49.

(33) (a) Wu, Y. Y.; Wong, D. S. H.; Tan, C. S. *Ind. Eng. Chem. Res*. **1991**, *30*, 2492. (b) Larin, A. V.; Frolova, E. A. *Colloid J.* **1995**, *57*, 413.

(34) For example, see: (a) Oscik, J. In *Adsorption*; Cooper, I. L., translation ed.; John Wiley and Sons: New York, 1982. (b) Satterfield, C. N. *Heterogeneous Catalysis in Industrial Practice*, 2nd ed.; McGraw-Hill: New York, 1991.

(35) Tester, J. W.; Modell, M. *Thermodynamics and its Applications*, 3rd ed.; Prentice Hall: Upper Saddle River, NJ, 1997.